8464

NACA TN 2037

TECH LIBRARY KAFB, NM
0065368

NATIONAL ADVISORY COMMITTEE FOR AERONAUTICS

TECHNICAL NOTE 2037

RESISTANCE OF SIX CAST HIGH-TEMPERATURE ALLOYS TO CRACKING CAUSED BY THERMAL SHOCK

By M. J. Whitman, R. W. Hall, and C. Yaker

Lewis Flight Propulsion Laboratory
Cleveland, Ohio

Washington
February 1950

AFMDC
TECHNICAL LIBRARY
AFL 2811

TECH LIBRARY KAFB, NM

0065368

NATIONAL ADVISORY COMMITTEE FOR AERONAUTICS

TECHNICAL NOTE 2037

RESISTANCE OF SIX CAST HIGH-TEMPERATURE ALLOYS TO CRACKING CAUSED BY THERMAL SHOCK

By M. J. Whitman, R. W. Hall, and C. Yaker

SUMMARY

An investigation was undertaken to determine the relative resistance of six cast high-temperature alloys to cracking caused by thermal shock. The thermal-shock evaluation unit utilized a controlled water quench of the symmetrical edge of a uniformly heated, modified wedge-shaped specimen. The specimens were heated at a uniform temperature of 1750° F for 1 hour and water quenched at 45° F. This cycle was repeated until thermal-shock failure occurred. The order of decreasing resistance to thermal-shock cracking of the alloys was S-816, S-590, Vitallium, 422-19, X-40, and Stellite 6.

The heating-and-quenching cycle produced elongation of the quenched edge. Measurements of these deformations were made during the cyclic tests. The total elongation of the quenched edge at failure was found to increase with the resistance of the material to thermal shock. In this investigation, materials having similar thermal properties, such as coefficient of linear expansion, conductivity, and specific heat, were shown to have widely differing resistances to thermal shock. Metallurgical examination of the alloy structure and study of the nature of crack propagation yielded no correlation between structural characteristics and resistance to cracking caused by thermal shock.

An analysis of the manner in which the thermal-shock crack formed and progressed into the specimen and an examination of available data on the notch impact strength of cast high-temperature alloys indicated that there might be a relation between notch impact strength and resistance to cracking caused by thermal shock.

INTRODUCTION

The operating conditions of aircraft gas turbines subject certain components to large and sudden temperature gradients, which result in thermal stresses that are, in some cases, either a prime or contributing cause of component failure. For example, gas-turbine blades are subjected to thermal stresses when the engine is started, accelerated, decelerated, or stopped. Rapid cooling of the turbine-blade edges during deceleration and stopping causes contraction of these thin sections. This contraction is resisted by the adjacent hotter metal and as a result the cooler edges are subjected to sudden tensile stresses. Rapid heating produces compressive stresses in the same areas.

Observations made at the NACA Lewis laboratory indicate that certain gas-turbine components fail in tension as a result of thermal stresses or fail after cracks have been caused by these stresses. These observations indicate that one criterion in selecting a high-temperature turbine material may be its ability to withstand tensile stresses produced by sudden localized cooling from an elevated temperature.

Previous laboratory evaluations of alloys for high-temperature use in jet engines have consisted in determining stress-rupture, creep, fatigue, and corrosion-resistant properties. The few attempts that have been made to appraise the thermal-shock resistance of heat-resistant alloys have generally been of a qualitative nature. An exigency exists for a standard means of evaluating the susceptibility of gas-turbine materials to cracking caused by thermal shock.

The primary purpose of the investigation reported herein was to evaluate the relative resistance of six high-temperature alloys to thermal-shock cracking, which hereinafter is called thermal cracking.

The thermal properties, coefficient of linear expansion, thermal conductivity, and specific heat, have been accepted as factors relevant to the ability of materials to resist thermal shock (references 1 and 2). Experimental evaluation of thermal-shock resistance should make possible a comparison of the relative importance of thermal and mechanical properties in determining thermal-cracking resistance of alloys. Impact strength as well as tensile properties are considered because the manner in which the temperature gradient is induced results in rates of loading considerably greater than those encountered in normal tensile tests.

1224

The six cast alloys investigated, S-816, S-590, Vitallium, 422-19, X-40, and Stellite 6, have been used or considered for use in gas-turbine and other high-temperature applications. The alloy specimens were uniformly heated to 1750° F and then stressed by producing a thermal gradient with a controlled water quench at 45° F. Both specimen cracking and deformation produced by thermal shock were investigated.

Metallurgical examinations of the alloys before and after thermal-shock cycling were made to determine the manner of propagation of the cracks and the effect of the shock cycle on the structure of the alloys.

APPARATUS AND PROCEDURE

Resistance to thermal cracking was determined for the following cast alloys: S-816, S-590, Vitallium, 422-19, X-40, and Stellite 6. The compositions of these alloys, as determined from chemical analysis of test specimens that had failed, are given in table I. All specimens used in this investigation were cast at this laboratory. The shape and the dimensions of the specimens selected are shown in figure 1. This design was chosen in order to provide a concentration of thermal stresses during the cooling or quenching phase of the cycle. Quenching only the symmetrical edge of the specimen produces a large temperature gradient between this edge and the unquenched base of the specimen. The thermal stresses resulting from the temperature gradient are largest in the small cross-sectional area of the quenched edge. This edge is therefore most likely to crack. A finite edge width of 1/32 inch was selected in preference to a knife edge principally to minimize the effect oxidation might contribute to failure of the edge.

The quenching apparatus (fig. 2) was so designed that the narrow edge of the specimen was quenched in a stream of water, the flow rate and temperature of which were controllable. In order to minimize heat conduction from the specimen to the holder during quenching, the specimen was supported in such a manner that line contact was established between the holder and the two curved sides of the specimen (inset, fig. 2). Vertical adjustment of the specimen holder was provided by four machine screws, which also served as rigid supports for the holder. Misalinement of the specimen with the holder was negligible.

The essential features of the flow system through which the quenching water flows are also shown in figure 2. Tap water enters at the base of the quenching tank, passes through a cooling coil, and enters the base of the quenching trough. A horizontal baffle above the water inlet eliminates turbulence and assures a uniform overflow of water along the entire length of the trough. The quenching trough is equipped with a drain at each end; these drainage lines are closed during the quenching operation. 1224

The flow rate of the quenching water is controlled by a pressure-regulating valve placed in the inlet line of the quenching tank. The flow rate is measured by closing the valve in the quenching-trough drain and measuring the rate of flow of water from the sampling tube. The flow rate selected for the quench was the highest at which the level of water above the edge of the trough was uniform. Higher flow rates resulted in an uneven or bubbling flow of water from the trough. The level of the specimen holder was so adjusted that the symmetrical edge of the specimen just contacted the water.

Temperature of the quenching water was controlled by maintaining a constant temperature in the bath in which the cooling coil is located. The temperature of the bath was adjusted by adding solid carbon dioxide as required.

The specimens, placed in V-shaped grooves notched in a soft refractory brick resting on the hearth of the furnace, were heated in a small wire-wound resistance furnace. Special tongs, which gripped only the base edges of the specimen, were used to transfer the specimens from furnace to quenching trough.

Selection of experimental conditions to be used in the thermal-shock cycles was based on consideration of the following objectives:

1. Simulation, as nearly as possible, of conditions that might be encountered in aircraft-engine components

2. Attainment of conditions sufficiently severe to insure failure within a reasonable time period

3. Avoidance of high furnace temperatures in order to prevent excessive oxidation and changes in the microstructure of the alloys

On the basis of these considerations, a furnace temperature of 1750° F was chosen for the heating cycle. Temperatures in this range may be encountered for short periods of time in gas-turbine

1224

blades during acceleration. An inert atmosphere was not used in the furnace, which further simulated engine operating conditions. In the procedure developed, the specimen was held at a furnace temperature of 1750° F for 1 hour to insure temperature equilibrium throughout the specimen. At the end of this period, the specimen was gripped in the special tongs and transferred to the specimen holder. The quenching-trough drain valve was immediately closed, causing the water to rise over the edges of the trough onto the narrow edge of the specimen. The temperature of the quenching water was controlled at 45° ±2° F and the flow rate at 680 ±10 cubic centimeters per minute.

When the specimen was cool, it was removed from the holder, the oxide film was carefully removed from the narrow edge, and this edge was microscopically examined for cracks. Because crack propagation was not identical for all the alloys, an arbitrary criterion for failure was defined as presence of an opening that extended across the entire width of the quenched edge. In some specimens cracks progressed slowly across the width of the edge, whereas in others cracks extended across the entire width as soon as they originated. Cycling of the specimens was continued after failure, as defined, to investigate deformation resulting from thermal cycling. The number of complete cracks present after each quench cycle was observed.

In addition to causing cracking, thermal stresses caused warping of the test specimens (fig. 3). In order to determine relative resistance of the various alloys to such deformation, measurements of the distortion were made after every two shock cycles. Distortion was determined by measuring the height of the segment formed by the base of the specimen and the line connecting its end points. Such measurements were made on an optical comparator to an accuracy of 0.0001 inch. Percentage elongation was calculated from the measured deformation at the time the first complete crack appeared.

If thermal diffusivity of alloys is to be calculated, the specific heat must be known. Because specific-heat values for the alloys investigated were unavailable, diffusivity values at 300° F were experimentally determined using the method of Forbes (reference 3). Validity of the method was checked using oxygen-free high-conductivity copper, SAE 1020 steel, and 347 stainless steel. Values of diffusivity computed from the manufacturers' data for these materials were higher than the experimentally determined values by 8.0 percent for the copper, 9.4 percent for the 1020 steel, and 6.5 percent for the 347 stainless steel. The error in

experimentally determined diffusivity values is not only consistent but less than the percentage variation in reported values for coefficient of linear expansion. Inasmuch as the values of both diffusivity and coefficient of linear expansion are used in one equation, which relates physical properties to resistance to thermal cracking, the accuracy of the results obtained from the equation will not be impaired because of the errors in diffusivity. 1224

Upon completion of the thermal-cracking experiments, a metallurgical examination of the failed specimens was made. The specimens were sectioned and examined using standard metallographic procedures. In particular, studies were made of grain size, location of cracks with respect to grain boundaries, and changes in microstructure resulting from repeated heating and cooling.

RESULTS

A tabulation of cycles to failure for all the specimens observed is presented in table II in order of decreasing resistance of the alloys to thermal cracking. Figure 4 presents the deformations of the various materials through successive cycles and figure 5 presents a comparison of the thermal-shock deformation characteristics of the six alloys. The deformation per cycle was found to decrease with successive shock cycles and to vary considerably among the alloys.

The cracks form as the result of tensile stresses applied at a very high rate of loading during the quench portion of the cycle. The cracks originate at an edge of the quenched surface and progress across the surface with repeated cycling. The number of cycles before cracking starts is greater and the rate of crack progression is smaller for the materials having superior resistance to thermal cracking.

Metallographic examination after cycling revealed that the specimens all had approximately the same grain size — varying from a coarse size of 100 per square inch at the center of the specimen to 1600 per square inch at the quenched edge. Although some evidence was found indicating that in certain instances a crack initiated at a grain boundary, the cracks were predominantly transcrystalline in their propagation (fig. 6). In general, the structures of the various materials were similar, consisting of complex carbides in a solid-solution matrix with varying amounts of aging precipitate.

DISCUSSION OF RESULTS

With the apparatus and the evaluation procedure developed during this investigation, the resistance to thermal cracking of heat-resistant alloys may be determined. The procedure facilitates obtaining the following:

1. Good reproducibility of data resulting from easily controlled conditions

2. A large variation in cycles to failure for different alloys permitting ready determination of relative resistance to thermal cracking

3. Deformation data that can be used for correlation with thermal and physical properties

The composite curves of deformation (fig. 5) give an indication of the relative resistance of the alloys to distortion caused by thermal stresses. The behavior of the materials is considerably different: S-590 and S-816 show the most deformation per shock cycle, Vitallium and 422-19 an intermediate amount, and X-40 and Stellite 6 the least. Although alloy 422-19 has a deformation magnitude similar to that of Vitallium, the average number of cycles to failure for 422-19 is about the same as for X-40. The curves are nonlinear for all the materials and indicate that initial shock cycles cause more deformation than ensuing shock cycles. A possible explanation of the concavity of the curves is that the yield point of a metal is raised by the strain hardening that results from applied thermal stress. Upon repetition of the same thermal stress, less plastic flow would be expected in the metal because it then has a higher yield point. The 1-hour heating period at 1750° F during each shock cycle may, however, anneal an appreciable portion of the strain hardening. After a few cycles, X-40 and Stellite 6 suddenly failed and did not appreciably deform when subjected to additional cycles, probably indicating that further application of the thermal stresses resulted in extension of the fracture without further plastic deformation.

Actual elongation of the narrow edge at time of failure was calculated from the deformation measurements. In calculating the elongation, the specimen was assumed to be warped as an arc of a circle. This assumption was justified by comparisons of the curvature of the specimens on an optical comparator against a circle of suitable radius. Calculations of total elongation at the surface

of the narrow edge at failure showed that the elongation was in all cases less than would have been expected in a room-temperature tensile test. This apparent lowering of ductility may result from the higher rate of loading of the thermal-shock cycles.

From an examination of figure 7, the materials that show the greatest elongation at failure also resist the greatest number of cycles before failure, indicating that a relation exists between shock ductility (the ability to deform under sudden loads) and resistance to thermal cracking.

The factors that may contribute to the thermal-cracking resistance of a material may be divided into two classes: thermal and mechanical properties. In a previous investigation (reference 1) of the effects of a temperature gradient resulting from the sudden cooling of a uniformly heated body, the equation

$$\sigma = E\alpha\, dt = \frac{E\alpha\, K\, dx}{h} \tag{1}$$

was developed from the assumption that $dt/dx \propto 1/h$ and from the equation E = stress/strain.

The symbols used in equation (1) and the subsequent discussion are defined as follows:

C	heat capacity, (Btu/(lb)(°F))
dt/dx	thermal gradient
E	Young's modulus, (lb/sq in.)
E_d	ductility modulus, (lb/sq in.)
h^2	diffusivity, $\frac{k}{\rho C}$, (sq ft/hr)
K	constant
k	thermal conductivity, (Btu/(hr)(sq ft)(°F/ft))
n	number of cycles to failure
r^2	coefficient of determination
S_t	tendency to break

t temperature, (°F)

x distance from surface, (in.)

α coefficient of linear expansion, ((in./in.)/°F)

ρ density, (lb/cu ft)

Σ_b elongation at time of failure (breaking strain), (in./in.)

σ stress, (lb/sq in.)

σ_b breaking stress, (lb/sq in.)

For nonductile materials that break without appreciable plastic deformation, the equation $\sigma_b = E\Sigma_b$ was combined with equation (1) in the following manner:

$$\frac{\sigma}{\sigma_b} = \frac{E\alpha\ K\ dx}{Eh\ \Sigma_b} = K\ dx\ \frac{\alpha}{h\Sigma_b} = S_t \tag{2}$$

In the investigation reported in reference 1, a correlation was found to exist between S_t and $\alpha/h\Sigma_b$ for a number of ceramic bodies. The same equation can be considered to apply to materials that show some plastic ductility before failure from thermal shock if the convention of "ductility modulus" (reference 4) is used. This convention states that the ductility modulus E_d is equal to ultimate stress divided by breaking strain. The parameter $\alpha/h\Sigma_b$ consists of a thermal property factor α/h and a mechanical factor $1/\Sigma_b$. Figure 7 is a plot on log-log coordinates of $1/\Sigma_b$ against cycles to failure for the six cast alloys and figure 8 is a similar plot of $\alpha/h\Sigma_b$ against cycles to failure. From these two figures, using standard statistical methods (reference 5), the lines of regression were computed and plotted, and the coefficients of determination were calculated. The coefficient of determination r^2 is a measure of the variance in one of two variables that is associated with the relation between the two variables. A value of r^2 of 1.00 indicates perfect association of one variable with another. It was found that for n against $1/\Sigma_b$, $r^2 = 0.953$ and for n against $\alpha/h\Sigma_b$, $r^2 = 0.963$. This approach to unity in values of r^2 indicates that in both cases a straight-line plot on a log-log scale of n against either $1/\Sigma_b$ or $\alpha/h\Sigma_b$ is

justifiable. The agreement also indicates very little improvement in correlation between n and $1/\Sigma_b$ with the introduction of the thermal factor α/h to the independent variable.

It may therefore be concluded that knowledge of the thermal properties, coefficient of linear expansion, thermal conductivity, and specific heat is unnecessary in determining the relative thermal-cracking resistance of the alloys. A plot of $1/\Sigma_b$ against n (fig. 7) defines with a high degree of accuracy the resistance to thermal cracking. The values of h and α used and the source of the α values are listed in table III. For qualitative comparison, equations were developed from the data in tables II and III for cycles to failure as a function of the reciprocal of the elongation at failure and of the thermal constant α/h times the reciprocal of elongation at failure. The equations, as determined by the method of least squares, are

$$n = 4198 \left(\frac{1}{\Sigma_b}\right)^{-1.318}$$

and

$$n = 0.002 \left(\frac{\alpha}{h\Sigma_b}\right)^{-1.370}$$

Although the magnitude of the stresses causing failure of these specimens is unknown, a qualitative explanation of crack formation and progression may be postulated. When the edge is suddenly quenched, it tends to contract rapidly. This contraction is restrained by the thicker portion of the specimen, which is still at an elevated temperature. The stresses set up by these opposing forces exceed the yield point of the material and plastic flow of the narrow edge results. Although the hotter metal underlying the narrow edge has a lower yield point, the stresses are not so concentrated in this region because of the larger cross-sectional area. Plastic flow of the narrow edge tends to relieve the stresses in this edge but leaves it elongated. As the rest of the specimen cools, it contracts in an attempt to attain its original size, but this contraction is restrained by the elongated narrow edge and the specimen warps. If the stresses in the quenched edge exceed the ultimate strength at the temperature of the edge, cracking will result. In most cases, cracks started at the intersections

of the quenched surface and the curved faces of the specimen and worked gradually across the face of the edge during successive cycles. Various stages of this process are apparent in figure 9.

1224

The greatest rate of cooling and therefore the most drastic shock conditions are found along the intersections of the quenched surface and the curved faces of the specimen. This factor combined with the presence of very small rough spots, nicks, and other flaws that can act as stress raisers results in the formation of small cracks at these corners. With repeated cycling, these cracks become larger until they progress completely across the quenched edge (fig. 9).

When the relation between the thermal-cracking resistance and the mechanical properties of a material is considered, it is necessary first to analyze the nature of the stress effects produced in the thermal shock. The sudden production of a temperature gradient in a material rapidly produces high stresses. The rate at which these stresses are produced is much higher than those encountered in normal tensile-testing procedures. The thermal stresses so produced cause rapid deformation and final failure by cracking. The nature of the crack propagation in this investigation was such that after the cracks began, the stressed edge of the material can be considered notched. The thermal-shock evaluation therefore consists of repeated rapid applications of load, which produce stresses that are increased by a notch effect as the specimens approach failure.

Because the nature of the thermal-shock cycle is such that the edge is near bath temperature while the heavy portion of the specimen is near furnace temperature, it may be postulated that the failure of the edge occurs at approximately room temperature. If this assumption is correct, it would be expected that a room-temperature test that approximates the stress conditions in thermal shock could be correlated with the thermal-cracking resistance of a material. Of all the room-temperature tests, the impact test most nearly resembles the thermal-shock test because of the high rate of loading and presence of the notch effect. The impact test should therefore yield data that can be related to thermal-cracking resistance. Tables II and III indicate that, in general, the alloys with the highest impact strength are those that have the greatest thermal-cracking resistance. The impact strength of an alloy may therefore be some indication of its thermal-cracking resistance.

The results of the metallurgical examination indicated that the alloys were similar in grain size. All the alloys aged during heating, the amount of precipitation increasing with increased time at temperature. The cracks were generally transcrystalline in propagation and it therefore appears that grain size is an unimportant factor in determining thermal-cracking resistance. Perhaps the most probable reason for the differences among samples of each alloy is the random orientation that is present in cast coarse-grained alloys of this type. Because all the alloys are similar in their structural behavior, the order of merit obtained in this investigation might apply at lower evaluation temperatures, that is, only the magnitude (number of cycles to failure) of the thermal-cracking resistance of each alloy would change with temperature.

1224

SUMMARY OF RESULTS

An investigation was conducted to determine the relative resistance of six cast heat-resisting alloys to thermal cracking caused by repeated thermal stresses.

The order of decreasing resistance to thermal cracking of specially designed alloy specimens was S-816, S-590, Vitallium, 422-19, X-40, and Stellite 6. The materials with the greater shock ductility (the ability to deform under sudden loads) survived the greater number of shock cycles. Too few data, however, were available for accurate quantitative statement of the relation.

Materials having similar thermal properties (coefficient of linear expansion, thermal conductivity, and specific heat) were shown to have widely different resistances to thermal shock.

Metallurgical examination of the alloy structures and a study of the nature of crack propagation led to the conclusion that structural characteristics of the alloys were insignificant in defining resistance to thermal cracking.

The limited available data on notch impact strength of cast high-temperature alloys indicated a possible relation between notch impact strength and resistance to thermal cracking.

Lewis Flight Propulsion Laboratory,
National Advisory Committee for Aeronautics,
Cleveland, Ohio, July 22, 1949.

1224

REFERENCES

1. Norton, F. H.: Refractories. McGraw-Hill Book Co., Inc., 2d ed., 1942, p. 470.

2. Avery, Howard S., and Wilks, Charles R.: Cast Heat Resistant Alloys of the 26% Chromium-20% Nickel Type – Part I. Trans. A.S.M., vol. 40, 1948, pp. 529-577; discussion, pp. 577-584.

3. Cork, James M.: Heat. John Wiley & Sons, Inc., 2d ed., 1942, p. 121.

4. Lidman, W. G., and Bobrowsky, A. R.: Correlation of the Physical Properties of Ceramic Materials with Resistance to Fracture by Thermal Shock. NACA TN 1918, 1949.

5. Hoel, Paul G.: Introduction to Mathematical Statistics. John Wiley & Sons, Inc., 1947, pp. 78-89.

6. Kittel, J. Howard: Comparison of Crystal Structures of 10 Wrought Heat-Resisting Alloys at Elevated Temperatures with Their Crystal Structures at Room Temperatures. NACA TN 1488, 1947.

7. Anon.: Metals Handbook, 1948 Edition. Am. Soc. Metals (Cleveland, O.), 1948, p. 579.

8. Grant, Nicholas J., Frederickson, A. F., and Taylor, M. E.: A Summary of Heat Resistant Alloys from 1200° to 1800° F. Iron Age, vol. 161, no. 12, March 18, 1948, pp. 73-78.

9. Anon.: Symposium on Materials for Gas Turbines. Am. Soc. Testing Materials (Philadelphia), 1946.

TABLE I - COMPOSITION OF ALLOY SPECIMENS AS DETERMINED

BY CHEMICAL ANALYSES

Alloy	C	Cr	Ni	Co	Mo	W	Cb	Fe	Si
S-816	0.30	18.06	20.80	43.80	4.07	3.74	3.51	2.72	---
S-590	.31	19.17	20.32	19.65	4.27	3.82	3.80	25.39	---
Vitallium	.3	27.0	2.7	61.1	5.8	----	----	1.5	---
422-19	.4	25.4	15.6	49.1	6.3	----	----	1.3	---
X-40	.5	25.1	11.2	54.2	----	7.6	----	.6	0.3
Stellite 6	.93	28.6	.5	62.2	----	5.4	----	.7	.3

1224

TABLE II - RESISTANCE OF ALLOYS TO THERMAL CRACKING

Alloy	Specimen	Cycles to failure
S-816	A	86
	B	104
	H	105
S-590	A	34
	D	34
	E	36
Vitallium	D	24
	W	30
422-19	V_1	6
	V_2	6
	V_3	8
X-40	A	7
	B	6
	D	7
	H	7
Stellite 6	B	2
	D	12
	E	4
	G	2
	Q	2
	U	2

TABLE III - PHYSICAL PROPERTIES OF ALLOYS INVESTIGATED

Alloy	Coefficient of linear expansion from 70° to 1600° F ((in./in.)/°F)	Diffusivity (sq ft/hr)	Tensile strength (lb/sq in.)		Percentage elongation in 2 inches during room-temperature tensile test	Charpy V-notch impact strength at 70° F (ft-lb)
			70° F	1200° F		
S-816	[a]9.02×10^{-6} [f]8.53 [g]9.90 [d]9.4	[b]0.16	[c]100.0×10^{3} [d]112.0		[d]5 [c]6.0	[b,e]4.7
S-590	[g]9.20×10^{-6} [a]9.22 [d]9.20	[b]0.16				[b,e]3.2
Vitallium	[d]8.72×10^{-6}	[b]0.22	[c]101.3×10^{3} [f]101.3 [d]110.0	[d]71.0×10^{3} [f]86.2	[d]10 [c]8.2 [f]8.2	[g]2.9
422-19	[d]8.54×10^{-6} [f]8.54	[b]0.20	[d]98.1×10^{3} [c]98.1 [f]98.1	[d]58.3×10^{3} [c]59.9	[d]5.0 [c]5.0 [f]5.0	[g]1.5
X-40	[d]8.79×10^{-6} [g]8.86	[b]0.19	[c]101.0×10^{3} [d]101.0	[d]76.8×10^{3} [c]80.1	[d]11 [c]11.0	[g]2.3
Stellite 6	[f,h]8.45×10^{-6}	[b]0.19	[f,h]105.4×10^{3} [d,h]103.4	[d,h]79.5×10^{3} [c,h]82.9	[d,h]7 [c,h]7.0	[g,h]2.4

[a]Reference 6.
[b]Experimentally determined at NACA Lewis laboratory.
[c]Reference 7.
[d]Reference 8.
[e]Ingots held 21 hr at 1725° F and air-cooled.
[f]Manufacturer's data.
[g]Reference 9.
[h]Data reported for alloy 61.

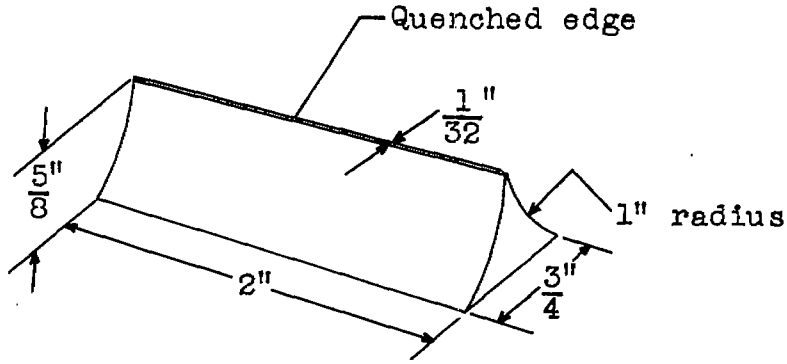

Figure 1. - Specimen for determining resistance to thermal cracking.

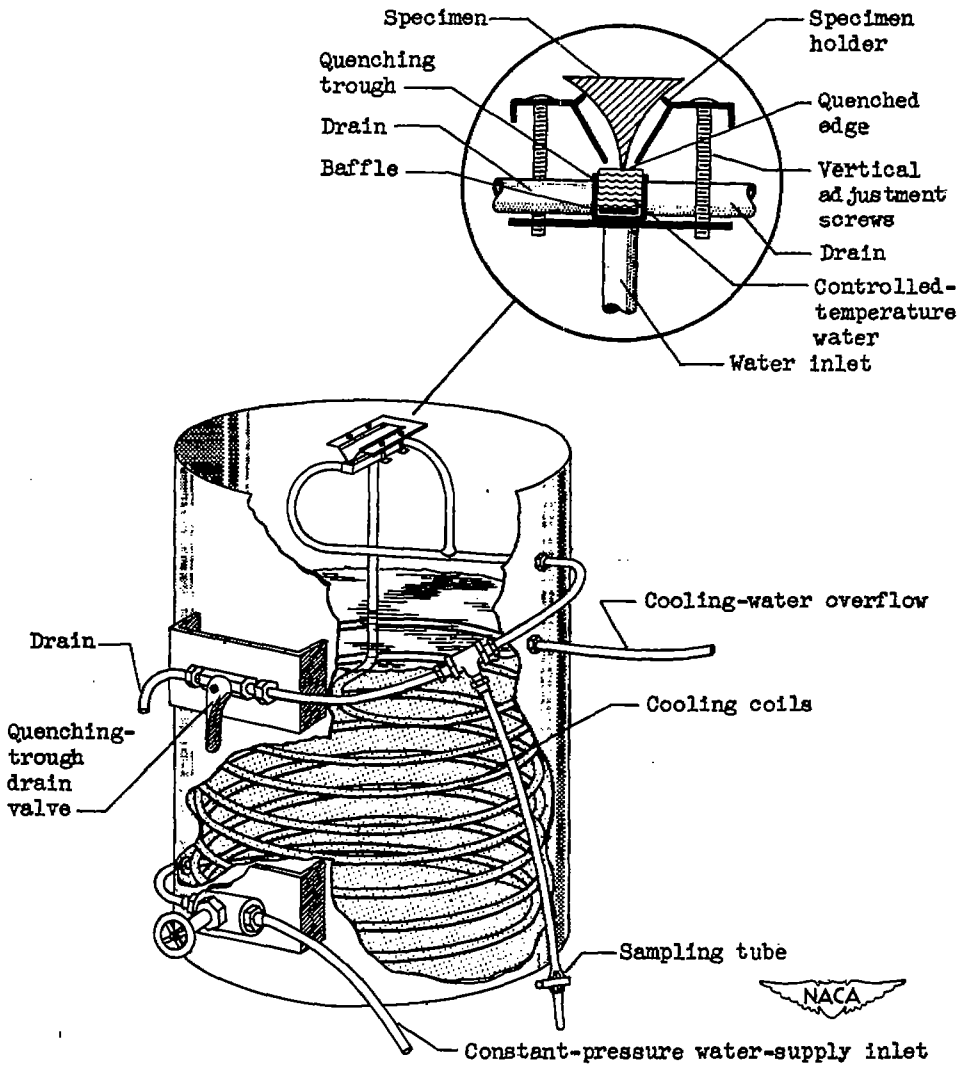

Figure 2. - Apparatus for quenching thermal-shock specimens.

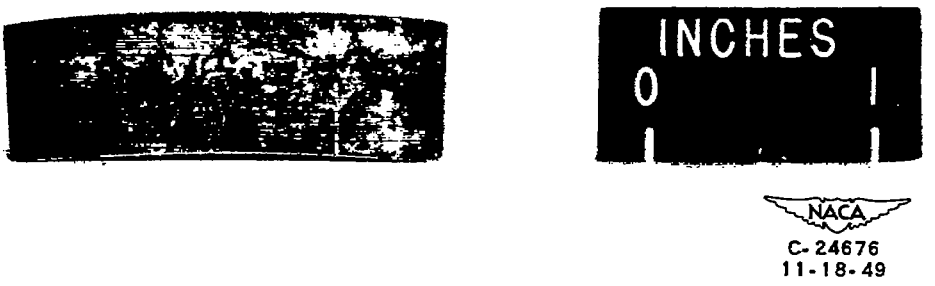

Figure 3. - Specimen after repeated thermal-shock cycles. Note curvature produced by thermal stress.

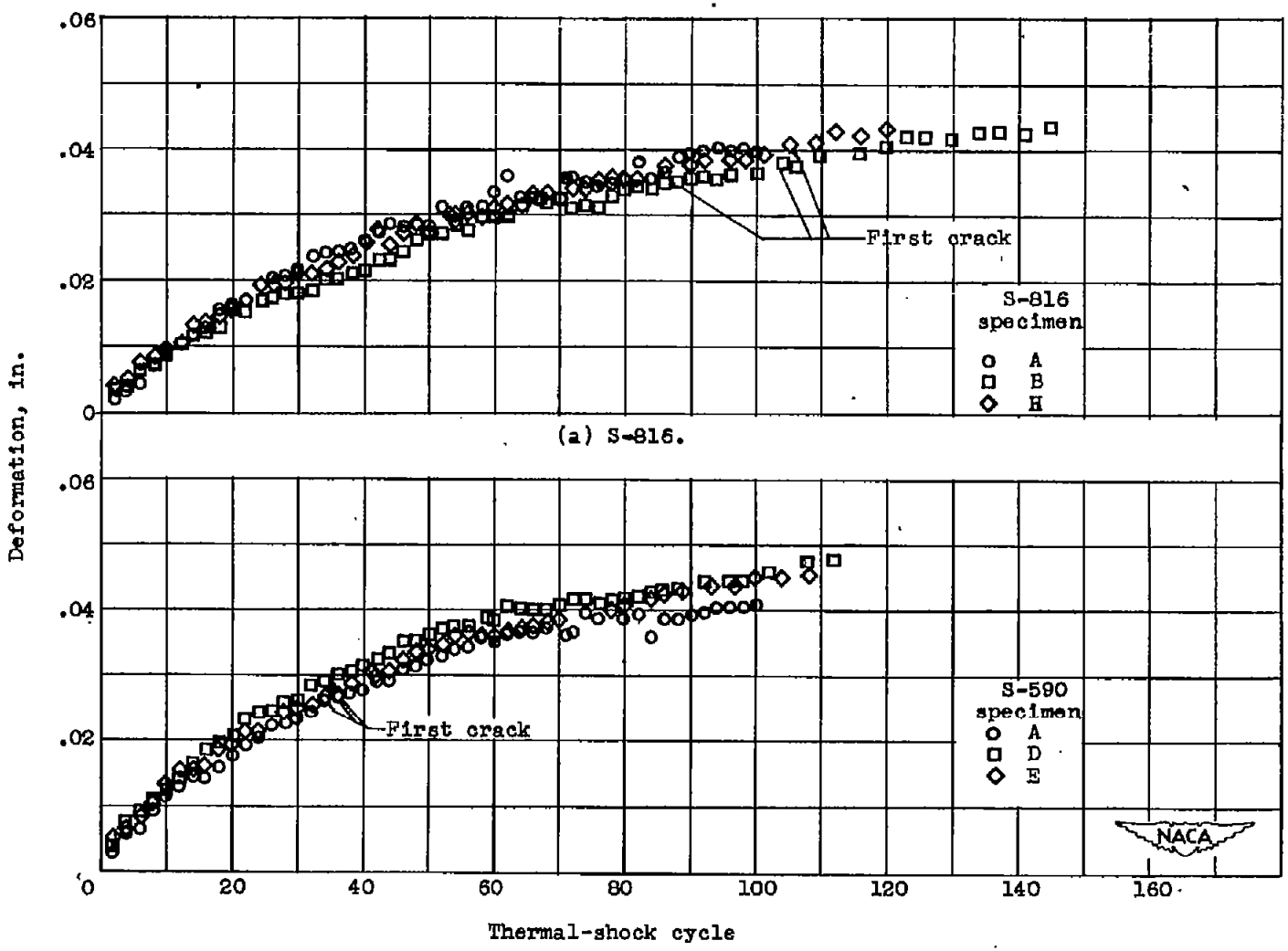

(b) S-590.

Figure 4. - Deformation produced in specimens by thermal shock.

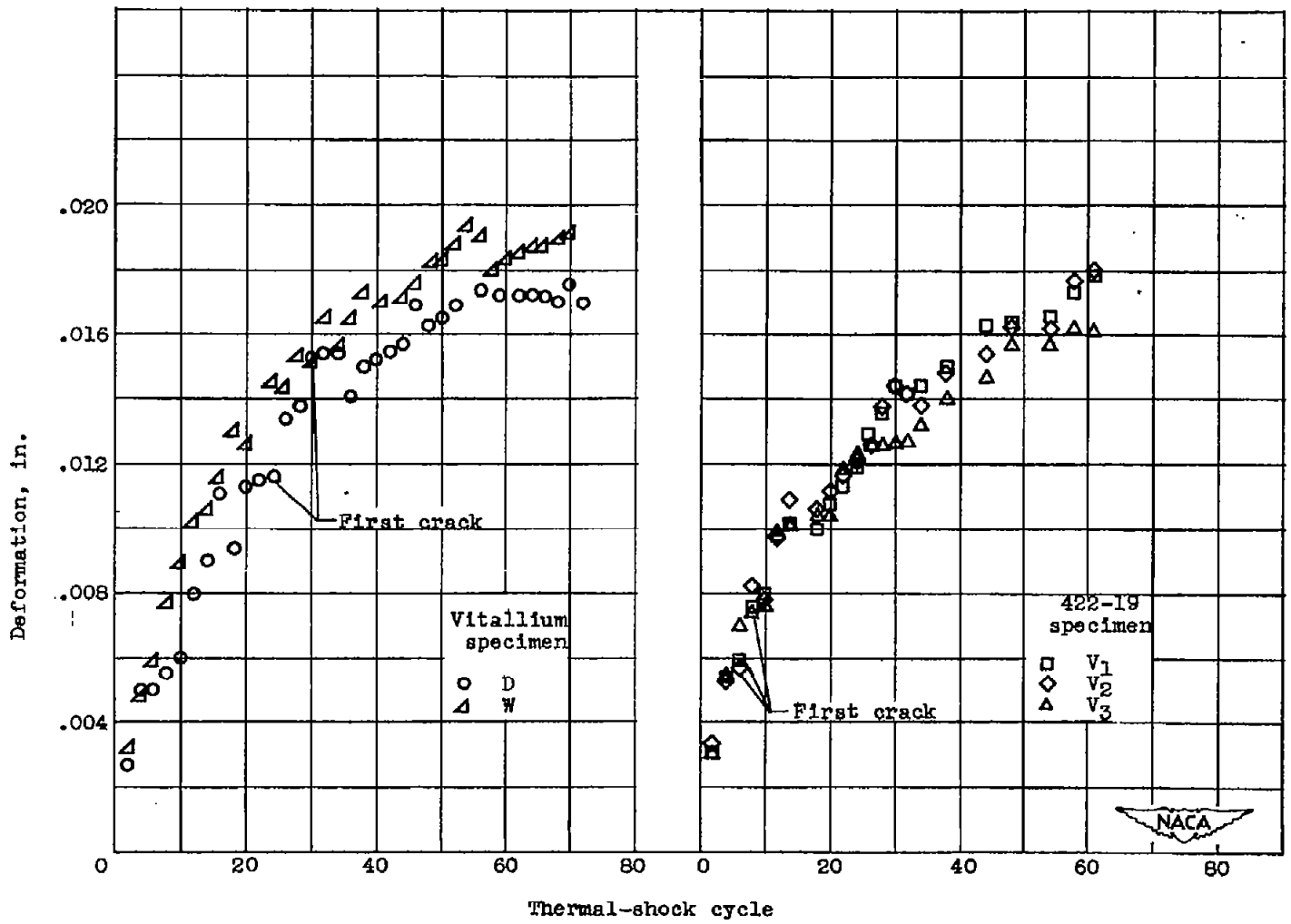

(c) Vitallium. (d) 422-19.

Figure 4. - Continued. Deformation produced in specimens by thermal shock.

1224

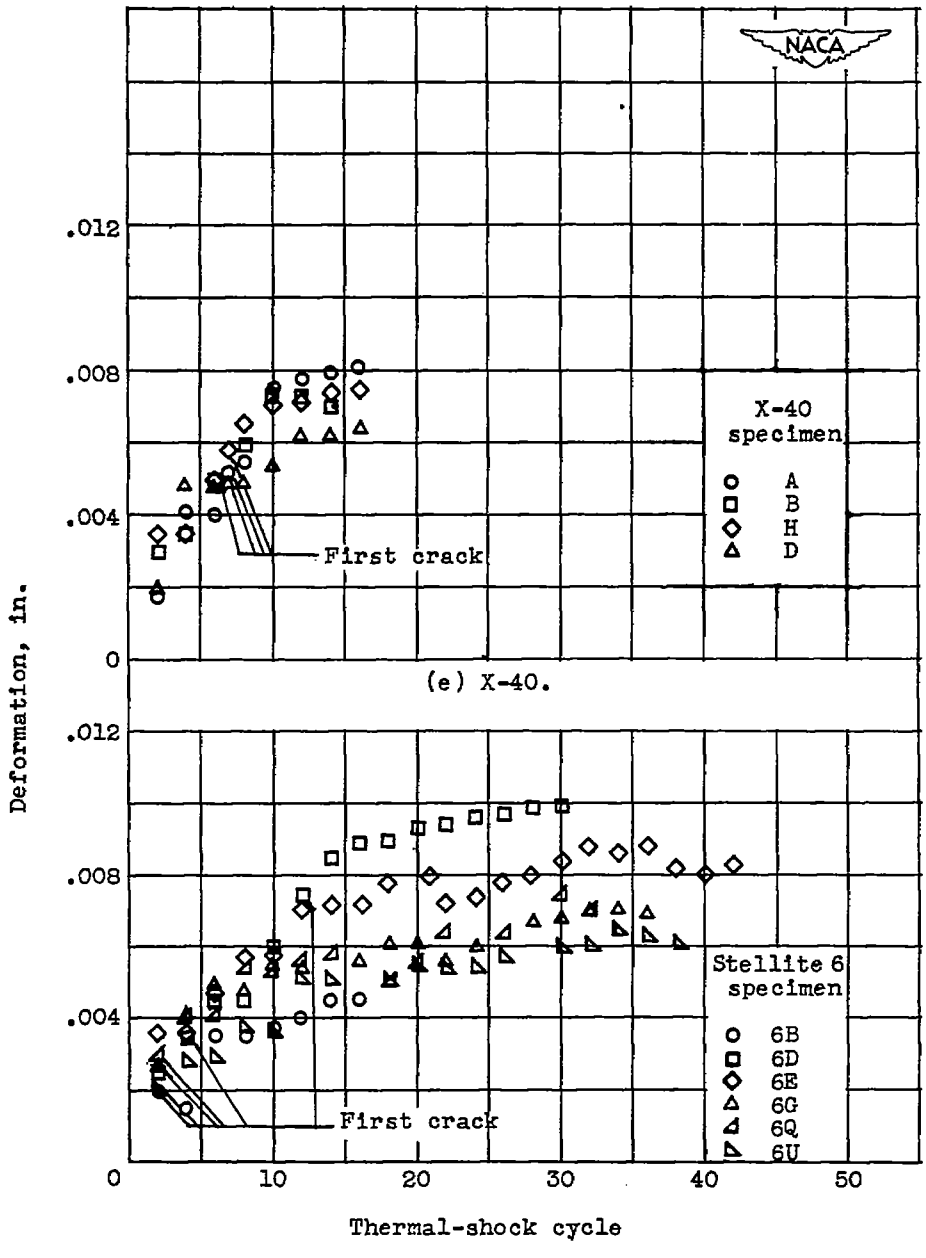

(f) Stellite 6.

Figure 4. - Concluded. Deformation produced in specimens by thermal shock.

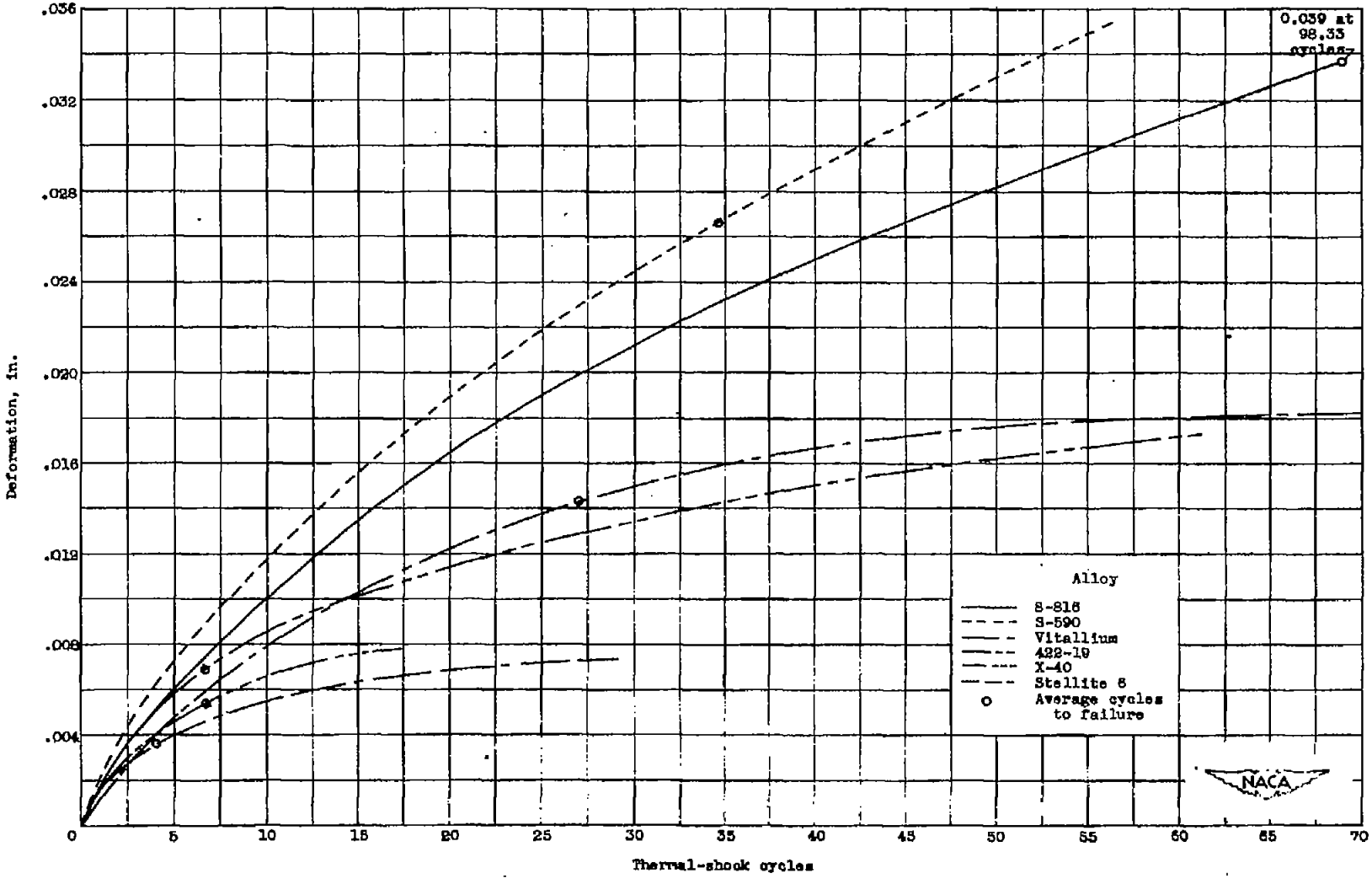

Figure 5. - Composite curves illustrating progressive deformation of specimens with repeated thermal shock.

1224

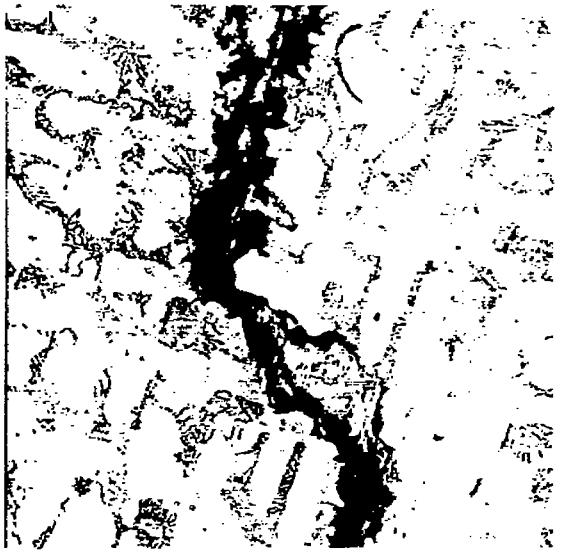

(a) S-816. Alloy matrix containing primary carbides in pearlitic-type dispersion plus fine precipitates. X250.

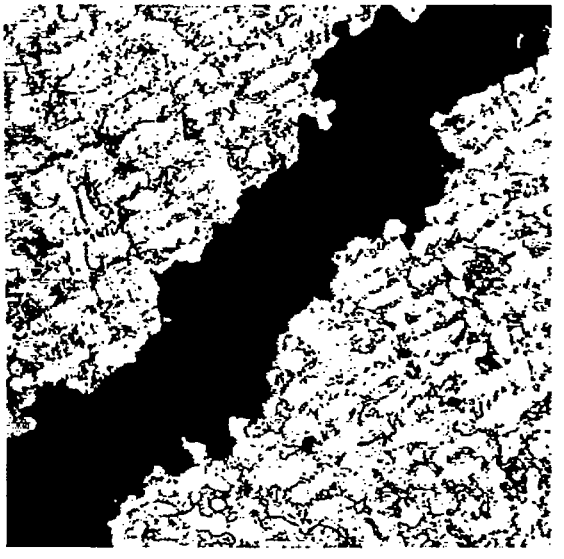

(b) S-590. Alloy matrix containing primary carbides in pearlitic-type dispersion and fine precipitate. X150.

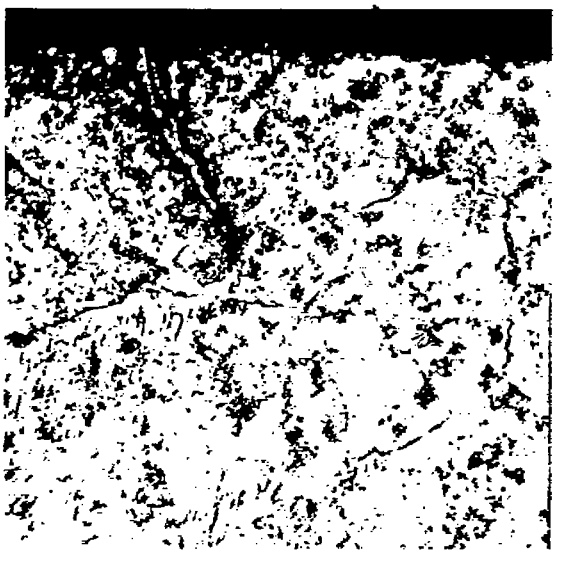

(c) Vitallium. General carbide precipitation and preferential precipitation along crystallographic planes. X250.

(d) 422-19. Primary carbides with heavy agglomerated precipitate. X250.

NACA
C-24832
12-6-49

Figure 6. - Microstructures of alloys in vicinity of cracks. (Varying magnifications used to reveal nature of crack propagation.) Electrolytically etched in 10-percent hydrochloric acid in ethyl alcohol.

1224

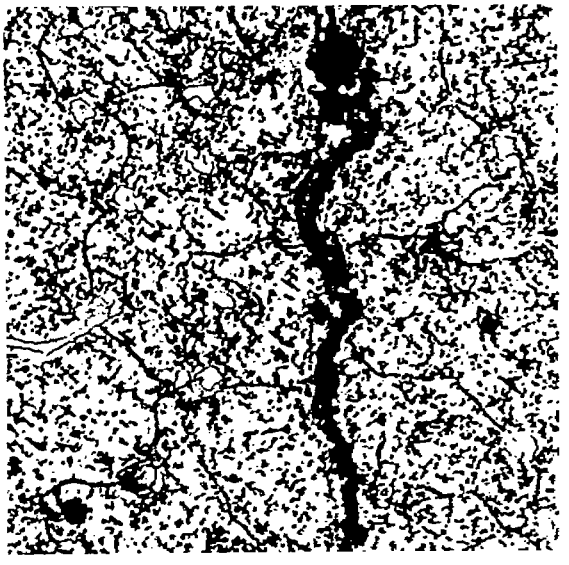

(e) X-40. Primary carbides with heavy agglomerated precipitate. X1000.

NACA
C-24833
12-6-49

(f) Stellite 6. Primary carbides with small amount of precipitate. X50.

Figure 6. - Concluded. Microstructures of alloys in vicinity of cracks. (Varying magnifications used to reveal nature of crack propagation.) Electrolytically etched in 10-percent hydrochloric acid in ethyl alcohol.

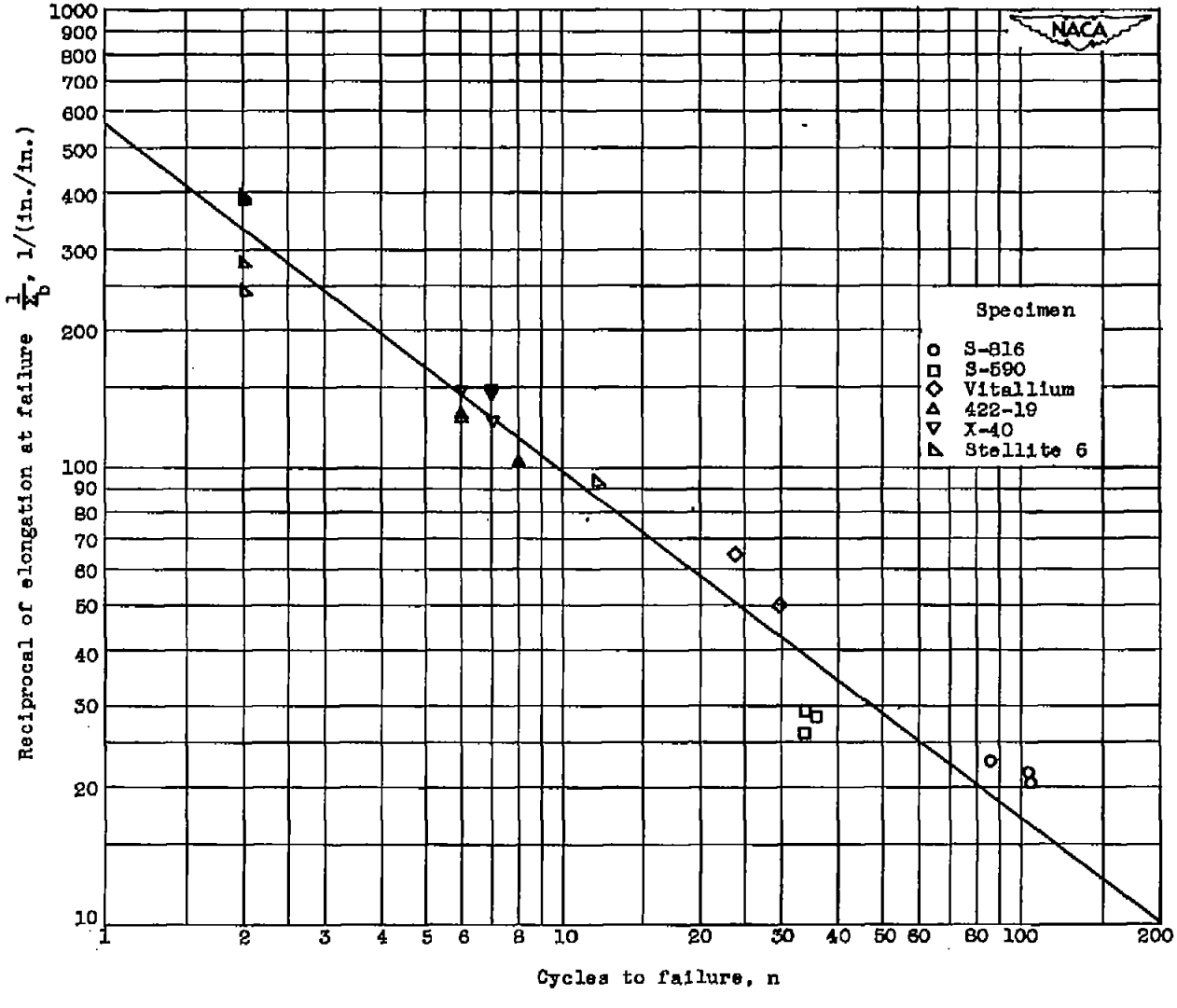

Figure 7. - Relation of reciprocal of elongation at failure to thermal-cracking resistance.

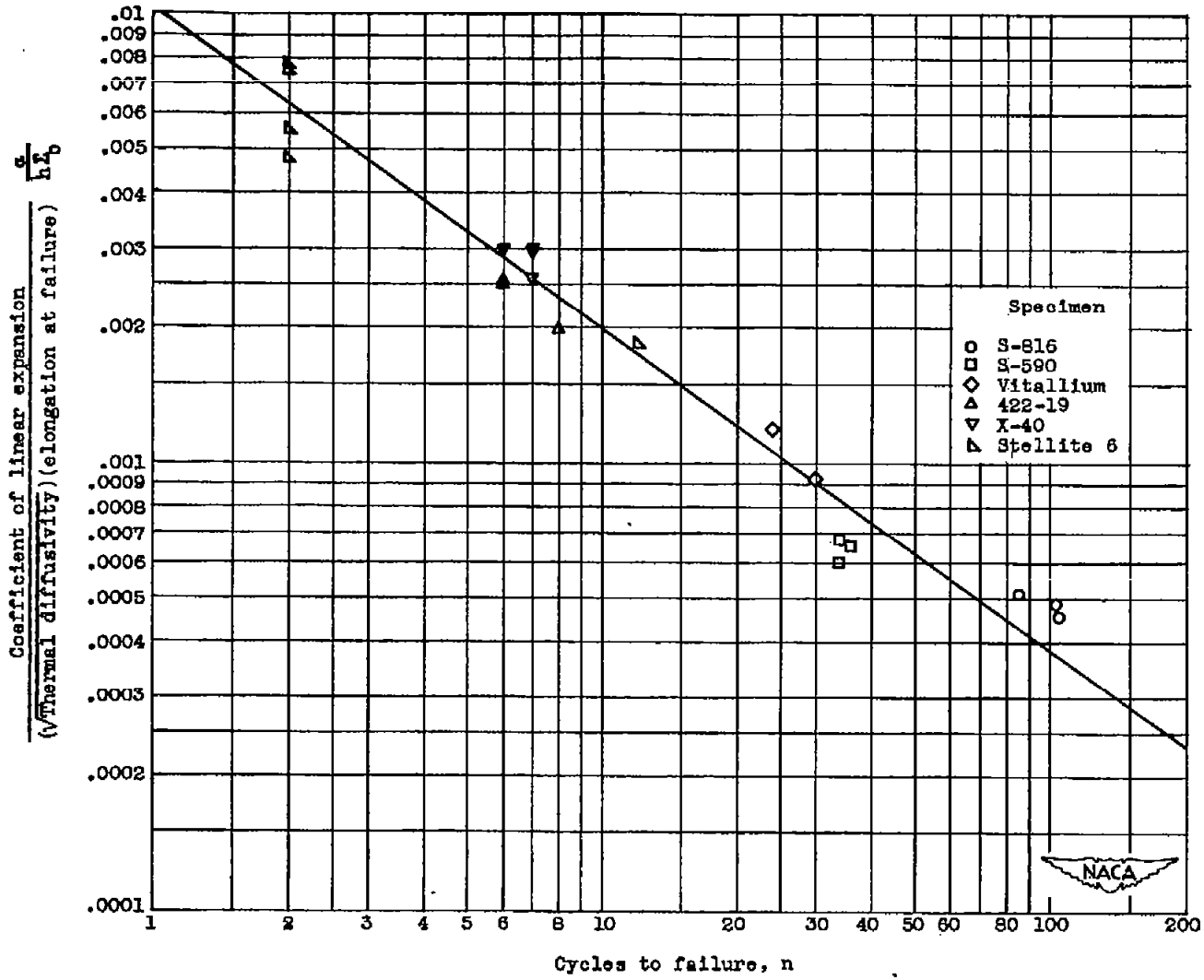

Figure 8. - Relation of reciprocal of elongation and thermal properties to thermal-cracking resistance.

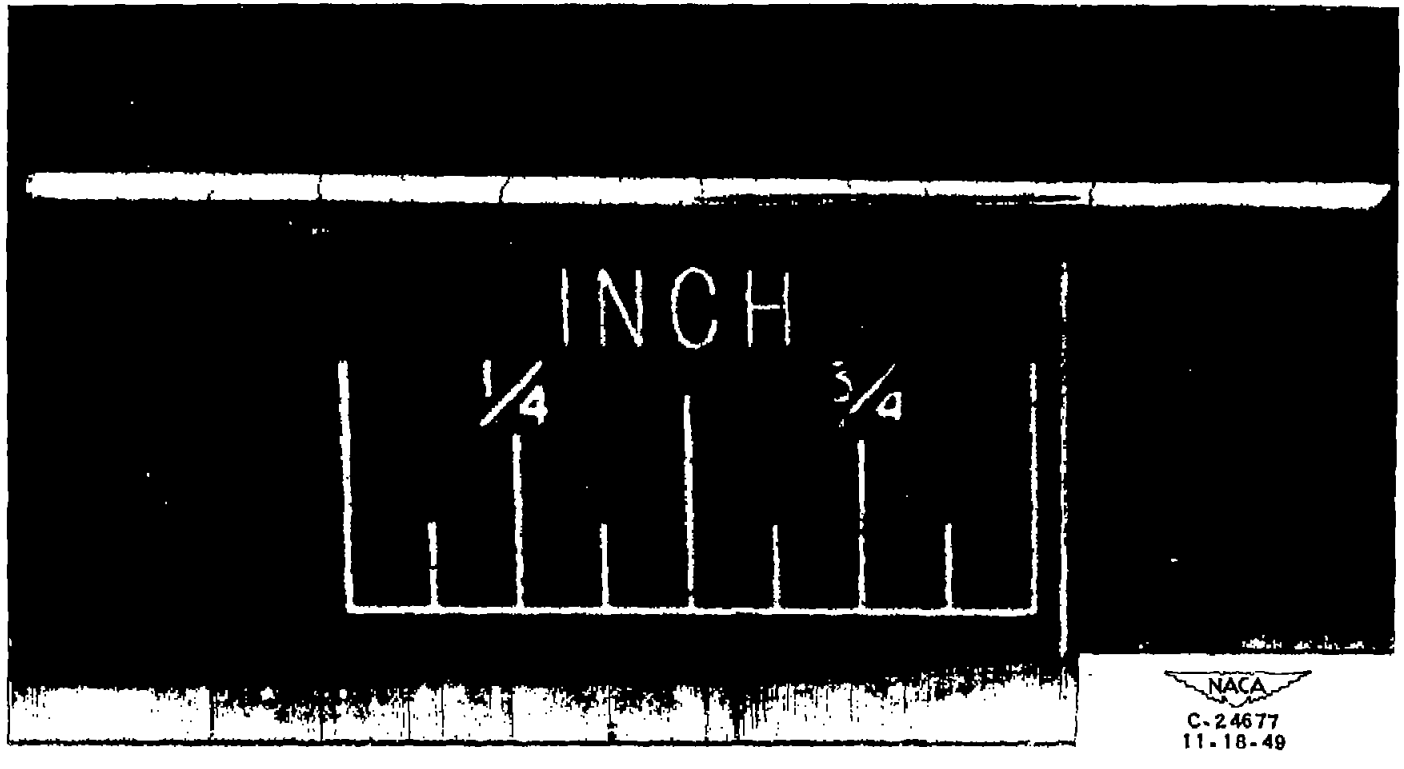

Figure 9. - Quenched symmetrical edge of S-590 specimen after 100 thermal-shock cycles.

NACA-Langley - 2-27-50 - 650